

Large aperture compound lenses made of lithium

J. T. Cremer,^{a)} M. A. Piestrup, H. R. Beguiristain, and C. K. Gary
Adelphi Technology Inc., 2181 Park Blvd., Palo Alto, California 94306

R. H. Pantell
Department of Electrical Engineering, Stanford University, Stanford, California 94305

(Received 4 June 2002; accepted 6 January 2003)

We have measured the intensity profile and transmission of x rays focused by a series of biconcave parabolic unit lenses fabricated in lithium. For specified focal length and photon energy lithium compound refractive lenses (CRL) have a larger transmission, aperture size, and gain compared to aluminum, kapton, and beryllium CRLs. The lithium compound refractive lens was composed of 335 biconcave, parabolic unit lenses each with an on-axis radius of curvature of 0.95 mm. Two-dimensional focusing was obtained at 8.0 keV with a focal length of 95 cm. The effective aperture of the CRL was measured to be 1030 μm with on-axis (peak) transmissions of 27% and an on-axis intensity gain of 18.9. © 2003 American Institute of Physics. [DOI: 10.1063/1.1556948]

I. INTRODUCTION

A series of N biconcave lenses can be used to achieve one- and two-dimensional (2D) focusing and imaging at x-ray photon energies.^{1–20} Cylindrical, spherical, and parabolic unit lenses have been used. These compound refractive lenses (CRLs) have small apertures (submillimeter diameters) but are capable of in-line focusing and imaging at x-ray wavelengths with accompanied intensity gain. The gain is defined as the ratio of the on-axis intensity at the CRL's image plane divided by the on-axis intensity at the same plane without the CRL.

As is discussed by Snigirev *et al.*, low- Z materials are the best choices for CRLs.⁴ Indeed, as suggested by Pereira and co-workers, lithium should be ideal.^{17–19} Two-dimensional focusing and imaging was accomplished by multiple unit lenses made of Al, Mylar, kapton, and Be.^{10–16} Pereira and co-workers^{17–19} have built and tested prototypes of Cederstrom's²⁰ one-dimensional, saw-tooth refractive lens (or alligator lens) using lithium (Li). The Li saw-tooth refractive lens was tested at 10 keV and yielded a one-dimensional gain of 3 (expected gain was 4.5). In the present submission, individual biconcave parabolic lenses ("coin lenses") of Li are stacked to form a CRL capable of focusing in two dimensions and achieving a larger aperture (1030 μm) and a higher gain (18.9) than any previously CRL for the source size (<1 mm), source distance (<20 m), and focal length (<1 m).

II. THEORY

Lithium has a larger δ/μ than other CRL materials below 20 keV, and especially below 10 keV with the δ/μ of lithium twice that of beryllium and sixfold larger than carbon (kapton). The decrement δ of the real part of the complex index of refraction results from the oscillation of atomic electrons that lead to the refractive effects, whereas μ repre-

sents the collision losses in these oscillations that lead to the absorptive effects. The complex refractive index of the CRL material is expressed by

$$n = 1 - \delta - i\beta. \quad (1)$$

The decrement δ represents the ability of the CRL material to bend x rays, and δ is calculated from the real part f_1 of the complex atomic scattering factor for the forward scattering direction $f(0) = f_1 + if_2$.^{21,22} Specifically, the decrement is given by $\delta = (f_1 r_e \lambda^2 \rho) / (2\pi)$ with ρ the CRL atom density, λ the photon wavelength, and with r_e the classical electron radius (2.82×10^{-15} m). Conversely, the imaginary part of the complex index of refraction, β , is responsible for the absorptive losses in the CRL, and is calculated from the imaginary part f_2 of the complex atomic scattering factor by $\beta = (f_2 r_e \lambda^2 \rho) / (2\pi)$. The linear attenuation coefficient μ can be calculated from β by $\mu = 4\pi\beta/\lambda$. Note μ can be measured experimentally from which β and f_2 can be calculated, and then f_1 calculated from f_2 via the Kramers–Kronig dispersion relationship, thus allowing the calculation of the decrement δ from f_1 .

It is known for visible optics²³ that the focal length of a series of N lenses in contact with each other is reduced by $1/N$. Thus, as shown in Fig. 1, x-ray CRLs with short focal lengths have been made using a linear array of N closely packed biconcave parabolic lenses with an on-axis radius of curvature R (and physical aperture diameter $2r_m$) made of low atomic number, Z , materials. The resulting focal length is given by

$$f = \frac{R}{2N\delta}. \quad (2)$$

For a biconcave parabolic lens the total thickness t of material in the compound system given by

$$t = N \left(d + \frac{r^2}{R} \right) \quad (3)$$

^{a)}Electronic mail: ted@adelphitech.com

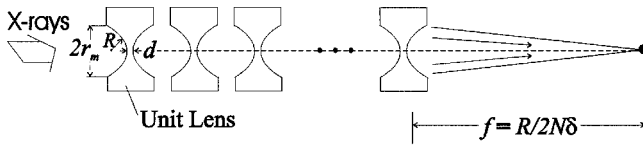


FIG. 1. X-ray focusing using compound refractive lens (CRL) comprised of a stack of N biconcave, parabolic unit lenses with on-axis radius of curvature R , minimum thickness d , and physical aperture diameter $2r_m$ fabricated from 0.020-in.-thick lithium foil. The individual lithium unit lenses has a focal length $f=R/2\delta$; however, the CRL has N -fold shorter focal length $f=R/2N\delta$.

increases as the square of distance r from the lens axis. Here, d is the minimum thickness of the unit lens. The aperture of x-ray CRLs is then limited by the attenuation increase in its outer radial portion. The lens is thicker at its periphery than its center. Hence, the path length through absorbing lens material is longer for trajectories at the lens periphery than its central portion. These effects make the compound refractive lens act like an iris as well as a lens. The attenuation radius, r_a , is defined as the value of the radial coordinate where there is an e^{-2} attenuation of the x-ray power through the CRL system. It is expressed as a function of the focal length f as^{4,11}

$$r_a = \left(\frac{4\delta f}{\mu} \right)^{1/2}, \tag{4}$$

where μ is the linear attenuation coefficient of the lens material. Equation (4) implies that the aperture attenuation radius r_a , and, consequently, other important CRL parameters such as resolution $\sim f\lambda/r_a$, and depth of focus, $\sim 1/r_a$, are solely determined by the required focal length f and the choice of material (δ/μ) of which the unit lenses are made. Figure 2 shows aperture diameter, D_a , as a function of photon energy for selected low- Z materials for CRLs of 1 m focal lengths, where $D_a \equiv 2r_a$. Figure 2 establishes for energies below 30 keV that CRLs assembled with Li and Be unit lenses achieve larger apertures than CRLs assembled with unit lenses formed with other materials.

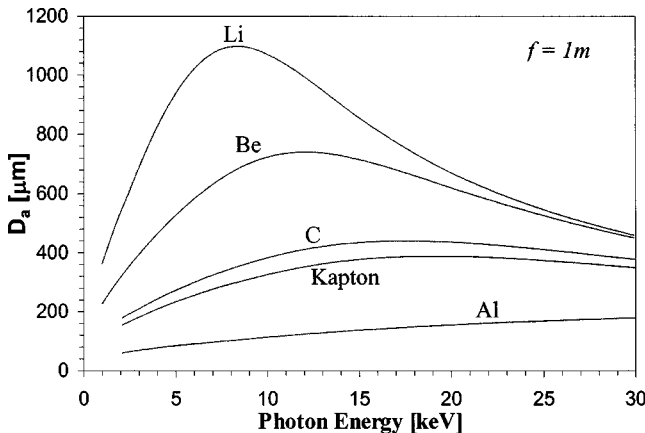


FIG. 2. CRL attenuation apertures as a function of photon energy for lenses with focal length of 1 m made of Li, Be, kapton, C, and Al. The figure establishes that x-ray CRLs assembled with Li unit lenses have about a factor of two larger apertures at the softer x-ray energy range of the figure (about less than 15 keV).

An application of CRLs is to increase the image intensity of a distant source (e.g., synchrotron). Recall the gain is defined as the ratio of the on-axis intensity at the CRL's image plane to the on-axis intensity at the same plane without the CRL. Using diffraction theory arguments, the gain of a two-dimensional lens is found to be¹¹

$$G = \left(\frac{r_0^2}{4\sigma_h\sigma_v} + fk^2 \frac{\delta}{\mu} \right)^{-1} \frac{(r_0k)^2}{\sigma_h\sigma_v} \left(\frac{\delta}{\mu} \right)^2 \exp(-\mu Nd) \approx \left(\frac{A_\epsilon}{A_s} \right) M^2 T. \tag{5}$$

Here, k is the photon wave number, σ_h and σ_v are the horizontal and vertical dimensions of the source, and r_0 is the object distance. The fraction of average power transmitted through the lens is $T \approx 0.43 e^{-\mu Nd}$. The full width half maximum (FWHM) aperture diameter is $r_a\sqrt{2\ln 2}$ and the FWHM aperture area of the lens is $A_\epsilon = \pi r_a^2 \ln 2/2$, A_s is the x-ray source FWHM area, and via $f \approx r_i$ the demagnification $M \approx r_0/f$.¹⁵

As can be readily seen from Eq. (5), there is a strong dependence of the gain on the choice of lens material (δ/μ). However, the gain is determined both by the parameters of the source and the distance between the source and CRL (A_ϵ, r_0) and the CRL (N, R), and not simply determined by the CRL material. Thus, the gain is not particularly good for comparing CRLs that do not share equivalent source area A_ϵ and object distance r_0 . For a fixed focal length f , the product of transmission T and attenuation radius r_a of the CRL is a better parameter for comparing lenses; i.e., $r_a T = 2\sqrt{f\delta/\mu} \exp(-\mu dR/2\delta f)$. As δ/μ increases the $r_a T$ product increases, and since lithium has the largest δ/μ for solid materials, lithium was used for fabricating the CRL. The unit lenses that we manufactured were biconcave and parabolic with on-axis radii of curvature of $R=0.95$ mm. The minimum lens thickness d , i.e., the minimum distance between parabolic refracting unit lens surfaces (as specified in Refs. 10–16) was measured to be $d=253 \mu\text{m}$. The lenses were compressed using techniques detailed in Ref. 13. The CRL being studied in this article was assembled with a stack of $N=335$ Li unit lenses. For Li the linear attenuation μ ranged from 0.8 cm^{-1} at 5 keV to 0.2 cm^{-1} at 9 keV and the real part of the refractive index δ ranged from 3.9×10^{-6} at 5 keV to 1.2×10^{-6} at 9 keV.

III. MEASUREMENTS

Experimental measurements were performed at the bending magnet beam line 2–3 on the Stanford Synchrotron Radiation Laboratory (SSRL). This beam line possessed a double-crystal Si(111) monochromator that was capable of delivering x rays from 2400 to 30 000 eV with a 5×10^{-4} resolution. The approximate FWHM source size²⁴ is $0.40 \times 1.7 \text{ mm}^2$. The experimental apparatus is shown in Fig. 3, and is the same as that specified in Refs. 10–16. The x-ray beam size was reduced to approximately $1.0 \times 1.0 \text{ mm}^2$ by tantalum (Ta) entrance slits (horizontal and vertical slits) upstream of the CRL. The lithium CRL was fabricated by compression molding technique¹³ in a dry environment.

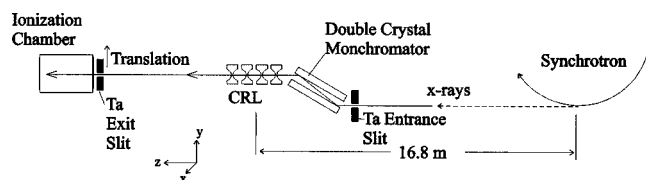


FIG. 3. Sketch of the experimental setup for testing the prototype Li CRL. X rays from a FWHM $400\ \mu\text{m} \times 1700\ \mu\text{m}$ bending magnet source at SSRL beamline 2–3 traverse 16.8 m through a Ta entrance slit and double crystal monochromator to the CRL entrance. The focused monoenergetic x rays from the CRL pass through a scanning Ta exit slit into a gas ionization detector. The exit slit scan in the vertical and horizontal directions yield the respective vertical and horizontal intensity profiles in the CRL image plane with and without the CRL present in order to experimentally determine the CRL gain.

The Li CRL was placed 16.8 m from the source in a goniometer head (not shown in Fig. 3), which could be manually tilted in two axes. The lens could also be translated orthogonally (x and y) to the direction of the x-ray beam. These adjustments maximize the x-ray transmission through the lens by aligning it with the beam.

An x-ray detector (ionization chamber) with a translatable Ta exit slit was used to profile the x-ray beam. The exit slit's width was adjusted to below $25\ \mu\text{m}$ by using a thin, stainless steel shim. It is likely the exit slit's jaws are not ideally parallel at these small dimensions. Consequently, the exit slit's width was minimally $>3\ \mu\text{m}$ when jaws appeared to be entirely closed. After adjusting its width, the exit slit was then translated in the x and y directions across the focused x-ray beam. The ionization chamber was downstream of the slits so that it measured the total x-ray power passing through it and, hence, when correlated with the slit's position, gave the beam's intensity profile (e.g., Fig. 5).

Various profiles of the x-ray beam along the propagation direction were obtained by placing the exit slit at different positions along the z axis of the x-ray beam. Vertical and horizontal widths were measured by scanning the horizontal and vertical slits, respectively, over the beam at each location

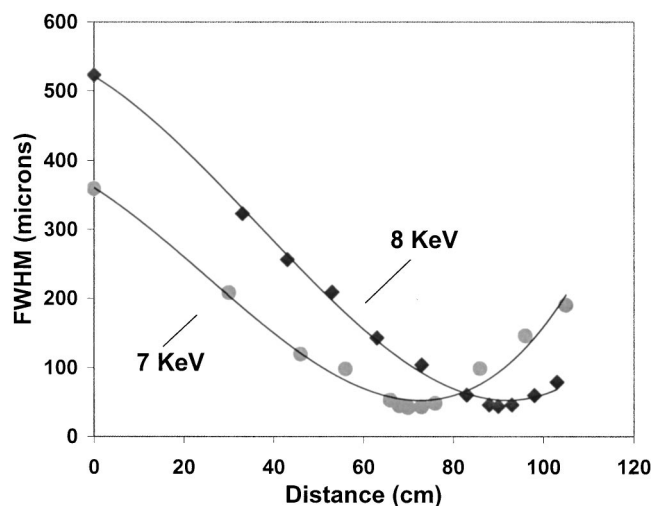


FIG. 4. Vertical profiles of 7.0 and 8.0 keV x rays focusing along the propagation direction. The minimum vertical FWHM of the image spots are 41.6 and $43.7\ \mu\text{m}$ at 70 and 90 cm, respectively, for the respective 7 and 8 keV photon energies.

TABLE I. Measured and calculated CRL parameters at 7.0 and 8.0 keV.

Object distance (m)	16.8	
Source vertical FWHM width (μm)	400	
Source horizontal FWHM width (μm)	1700	
Number of lenses in the CRL	335	
Parabolic lens on-axis radius of curvature (μm)	950	
Calculated lens minimum wall thickness (μm)	253	
Photon energy (keV)	7.0	8.0
Photon wavelength (\AA)	1.77	1.55
Tabulated real atomic scattering factor ^a	3.0	3.0
Calculated refractive index decrement	1.95×10^{-6}	1.50×10^{-6}
Tabulated linear attenuation coefficient ^a (m^{-1})	23.4	15.7
Calculated focal length (m)	0.73	0.95
Calculated image distance (m)	0.76	1.00
Measured image distance (m)	0.70	0.90
Calculated minimum waist diameter (μm)	18.1	23.8
Measured minimum waist diameter (μm)	41.6	43.7
Measured peak transmission (%)	9.7	26.3
Calculated attenuation aperture diameter (μm)	984	1200
Measured attenuation aperture diameter (μm)	667	1030
Calculated 2D gain	20.0	47.7
Measured 2D gain	3.84	18.9

^aReference 21.

in the z axis. The profile of the beam size as a function of distance from the lens was plotted using these measured widths. Figure 4 shows a series of vertical dimensions of the spot of 7.0 and 8.0 keV photons as a function of distance along the propagation direction from the Li CRL.

Table I displays the tabulated, calculated, and measured parameters for the Li CRL at 7.0 and 8.0 keV. The calculated and measured image distances for 7 and 8 keV are in fair agreement. However, the measured gain and peak transmission differ from their calculated values significantly due to lens surface roughness and distorted lens shape.

The measured image spot vertical profile has a $43.7\ \mu\text{m}$ FWHM at 8 keV and is displayed in Fig. 5. The image spot intensity profile is proportional to the transmission T of x

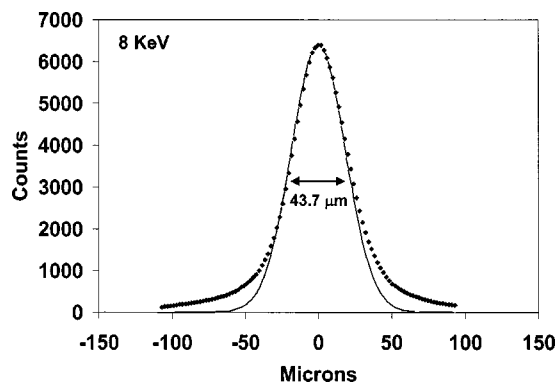


FIG. 5. Vertical profile of the 8.0 keV x-ray spot indicating the $43.7\ \mu\text{m}$ vertical FWHM produced by parabolic Li CRL at the image plane. The data are fitted with a solid line Gaussian distribution of $18.6\ \mu\text{m}$ standard deviation and $43.7\ \mu\text{m}$ FWHM about its mean, which is the center axis of the Li CRL.

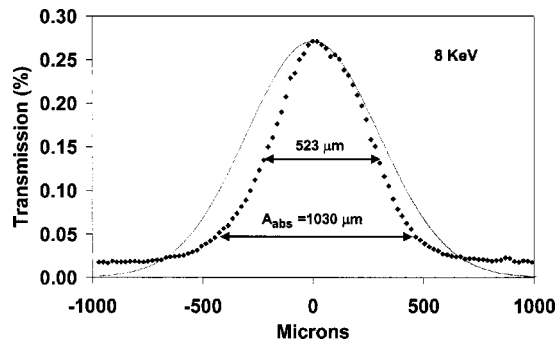


FIG. 6. Measured transmission through the CRL as a function of the radius of the lens. The figure shows the 1030 μm attenuation diameter of the lens as well as the 523 μm FWHM of the lens aperture. The solid line is the calculated transmission profile with an attenuation diameter of 1200 μm .

rays through the CRL and T varies as $\exp(-\mu Nt)$. Here, t is the thickness of the parabolic unit lens (and the x-ray path length through the unit lens) at distance r from the center axis common to the N unit lenses comprising the CRL. The measured 8 keV vertical profile in Fig. 5 is fitted with a Gaussian that has an 18.6 μm standard deviation and 43.7 μm FWHM about its mean, the center axis of the Li CRL. The deviation of the measured profile from the calculated Gaussian profile can result from (1) the transverse spatial distribution of the synchrotron electrons in the radiating bunch may not be Gaussian, (2) the angular divergence of the radiating synchrotron electrons may not be Gaussian, (3) the surface roughness of the lenses of the CRL can alter the transmission, and (4) the shape of the lenses of the CRL deviate from parabolic.

The measured FWHM spot size of the image, 43.7 μm is almost twice as large as would be expected from the geometric optics demagnification calculation of 23.8 μm . The latter can be attributed primarily to surface irregularities on the Li unit lenses. The rough surface of the Li CRL unit lens can be modeled as an array of protruding tiny 2D prisms on the unit lens surface. This array of tiny pyramid-shaped protrusions on the lithium unit lens tend to divergently refract the x rays away from the CRL center axis leading to larger FWHM image spot sizes than is expected with a smooth unit lens surface.

The stronger attenuation of the rays that pass through outer radial regions of the Li CRL results in the lens having an aperture with a Gaussian-shaped transmission profile. Since thickness t of the lens varies as $r^2/2R$ for the parabolic lens, the intensity transmission of x rays through the CRL varies with distance r from the CRL center axis as $T(r) = \exp(-\mu N r^2/2R)$. The transmission at the attenuation radius $r_a = \sqrt{2R/\mu N}$ is $T(r_a) = e^{-2}$ with FWHM transmission $T(r_a \sqrt{2 \ln 2/2}) = 0.5$. At 8 keV the intensity transmission as a function of distance $r(\mu\text{m})$ from the CRL axis varies as $T(r) = \exp(-r^2/2\sigma^2)$ with $\sigma = \sqrt{R/2\mu N}$ or $\sigma = 300 \mu\text{m}$ and $r_a = 600 \mu\text{m}$. The measured transmission across the Li CRL was obtained by translation of the lens across a very narrow $25 \times 25 \mu\text{m}^2$ x-ray beam. Figure 6 shows the measured profile of the transmission at 8 keV through the prototype Li CRL with the calculated profile. The Li CRL measured in this manner had a measured FWHM of 523 μm (or a mea-

sured attenuation diameter of $2r_a = 1030 \mu\text{m}$) and a measured peak transmission of 27%.

The intensity gain of the lens can be an effective measurement of the lens performance.⁴ The ratio of the intensity with the CRL in place divided by the intensity without the CRL yields the 2D gain. The 2D gain G_e was measured to be 18.9 at 8 keV, and the calculated 2D gain from Eq. (5) is 47.7. This discrepancy can be attributed to surface roughness on the lens, which can be modeled as a finite coherence length along the lens surface.²⁵

The measured spot size diameter D_e can be predicted from the measured 2D gain G_e . The calculated spot diameter $D_t = 23.8 \mu\text{m}$ is obtained by multiplying the demagnification (r_i/r_0) = 0.06 with the FWHM 400 μm vertical source dimension. That is, the predicted measured spot diameter is $D_e = D_t \sqrt{G_t/G_e} = 37.8 \mu\text{m}$. Given the actual spot size D_m measured in the experiment is 43.7 μm suggests a predicted slit width $W_t = \sqrt{D_m^2 - D_e^2} = 21.9 \mu\text{m}$, which is less than the 25 μm stainless-steel shim thickness used to set the Ta exit slit width and is thus a reasonable value.

Note the intensity gain is source distance, r_0 , and size dependent [see Eq. (5)]. If the same lens is placed on a beam line using a third-generation x-ray source, the gain of the CRL can be substantially increased. These sources can possess spot sizes that are a factor of ~ 113 times smaller (e.g., 0.02 by 0.3 mm^2). Also, typical distances from the insertion devices to the end stations can be ~ 60 m, compared to 16.8 m in our experiment. These longer object distances r_0 would consequently increase the gain by a factor of $(60/16.8)^2$ i.e., 12.7. For these source and placement parameters, the theoretical gain of Eq. (5) evaluated at 8.0 keV for this experiment's Li CRL would have been 6.8×10^4 . This gain results in a very sizable increase of the intensity from the case where no lens is utilized.

IV. DISCUSSION

For a specified focal length and photon energy below 30 keV, a Li CRL has a larger aperture than CRLs made with higher Z materials, such as Be, C, Al, etc. Also, higher gains are achievable with this Li CRL at the design energy and focal length than has been previously reported. The peak transmission of the lens, i.e., transmission along the lens axis, was found to be 27% at 8.0 keV. Decreasing the minimum wall thickness, d can further increase the transmission and the gain. The use of the CRLs at these x-ray energies can have wide application in synchrotron⁴⁻¹⁶ and novel²⁶ x-ray sources. For example, such CRLs could improve and enhance x-ray microscopy,⁹ x-ray diffraction, and medical imaging²⁷ techniques. Thus, one can expect compound refractive lenses made of Li unit lenses to have an important future in x-ray optics.

ACKNOWLEDGMENTS

This work was supported by the U.S. Missile Defense Agency under the Small Business Innovative Research Program managed under the U.S. Army Space and Missile Defense Command and was also supported by the California Trade and Commerce Agency administered by the Bay Area

Regional Technical Alliance. This work performed at the Stanford Synchrotron Radiation Laboratory, which is operated by the Department of Energy, Office of Basic Energy Sciences. The authors thank Dr. Nino Pereira for his suggestion that lithium would be a practical material for CRLs. The authors also thank Jeff Davis of Chemetall Foote Corporation of Kings Mountain, North Carolina, for providing lithium foil samples and for his advice on handling and fabrication techniques with lithium foil.

- ¹T. Tomie, Japan Patent No. 6-045288 (1994).
- ²T. Tomie, U.S. Patent No. 5,594,773 (1997).
- ³T. Tomie, U.S. Patent No. 5,684,852 (1997).
- ⁴A. Snigirev, V. Kohn, I. Snigireva, and B. Lengeler, *Nature (London)* **384**, 49 (1996).
- ⁵B. X. Yang, *Nucl. Instrum. Methods Phys. Res. A* **328**, 578 (1993).
- ⁶R. K. Smither, A. M. Khounsary, and S. Xu, *Proc. SPIE* **3151**, 150 (1997).
- ⁷A. Snigirev, B. Filseth, P. Elleaume, Th. Klocke, V. Kohn, B. Lengeler, I. Snigireva, A. Souvorov, and J. Tümmeler, *Proc. SPIE* **3151**, 164 (1997).
- ⁸B. Lengeler, J. Tümmeler, A. Snigirev, I. Snigireva, and C. Raven, *J. Appl. Phys.* **84**, 5855 (1998).
- ⁹B. Lengeler, C. G. Schroer, M. Richwin, J. Tümmeler, M. Drakopolulos, A. Snigirev, and I. Snigireva, *Appl. Phys. Lett.* **74**, 3924 (1999).
- ¹⁰J. T. Cremer, M. A. Piestrup, H. R. Beguiristain, C. K. Gary, R. H. Pantell, and R. Tatchyn, *Rev. Sci. Instrum.* **70**, 3545 (1999).
- ¹¹H. R. Beguiristain, M. A. Piestrup, R. H. Pantell, C. K. Gary, and J. T. Cremer, *Proceedings of the 11th Synch. Rad. Instr. Conference* (2000), Vol. 521, pp. 258–266.
- ¹²H. R. Beguiristain, J. T. Cremer, M. A. Piestrup, R. H. Pantell, C. K. Gary, and J. Feinstein, *Proc. SPIE* **4144**, 155 (2000).
- ¹³M. A. Piestrup, R. H. Pantell, J. T. Cremer, and H. R. Beguiristain, U.S. Patent No. 6,269,145 (2001).
- ¹⁴R. H. Pantell, J. Feinstein, M. A. Piestrup, H. R. Beguiristain, C. K. Gary, and J. T. Cremer, *Rev. Sci. Instrum.* **72**, 48 (2001).
- ¹⁵M. A. Piestrup, H. R. Beguiristain, C. K. Gary, J. T. Cremer, and R. H. Pantell, *Rev. Sci. Instrum.* **71**, 4375 (2000).
- ¹⁶H. R. Beguiristain, J. T. Cremer, M. A. Piestrup, C. K. Gary, and R. H. Pantell, *Opt. Lett.* **27**, 778 (2002).
- ¹⁷N. R. Pereira, D. A. Arms, R. Clarke, S. B. Dierker, E. Dufresne, and D. Foster, *Proc. SPIE* **4502**, 173 (2001).
- ¹⁸E. M. Dufresne, D. A. Arms, R. Clarke, N. R. Pereira, S. B. Dierker, and D. Foster, *Appl. Phys. Lett.* **79**, 4085 (2001).
- ¹⁹D. A. Arms, E. M. Dufresne, R. Clarke, S. B. Dierker, N. R. Pereira, and D. Foster, *Rev. Sci. Instrum.* **73**, 1492 (2002).
- ²⁰B. Cederström, R. Cahn, M. Danielsson, M. Lundqvist, and D. Nygren, *Nature (London)* **404**, 951 (2000).
- ²¹C. T. Chantler, K. Olsen, and D. S. Zucker (1999). *X-Ray Form Factor, Attenuation and Scattering Tables (version 2.0)* [2002, November 21]. (National Institute of Standards and Technology, Gaithersburg, MD, 2002), available: <http://physics.nist.gov/ffast>
- ²²E. M. Gullickson, *X-ray Data Booklet*, Center for X-Ray Optics and Advanced Light Source (2001), p. 144.
- ²³F. L. Pedrotti and L. Pedrotti, *Introduction to Optics* (Prentice-Hall, Englewood Cliffs, NJ, 1987), Chap. 3, p. 60.
- ²⁴H. Tompkins (private communication).
- ²⁵R. H. Pantell (unpublished).
- ²⁶M. A. Piestrup, H. R. Beguiristain, C. K. Gary, J. T. Cremer, R. H. Pantell, and R. Tatchyn, *Nucl. Instrum. Methods Phys. Res. B* **173**, 170 (2001).
- ²⁷B. Cederström, R. N. Cahn, M. Danielsson, M. Lundqvist, and D. R. Nygren, *Proc. SPIE* **3659**, 407 (1999).